

EUROPEAN COOPERATION  
IN THE FIELD OF SCIENTIFIC  
AND TECHNICAL RESEARCH

---

CA15104 TD(19)11004  
Gdansk, Poland  
2019/September./4-6

---

EURO-COST

---

SOURCE: (1) ESAT-TELEMIC,  
Katholieke Universiteit Leuven,  
Belgium

(2) RMI  
Belgium

## **A statistical study of atmospheric circumstances on microwave links.**

E. Van Lil  
KU Leuven  
Div. ESAT - Telemic  
Kasteelpark Arenberg, 10, box 2444  
B-3001 Heverlee (Leuven)  
BELGIUM  
Phone: + 32-16 32 11 13  
Fax: + 32-16 32 19 86  
Email: [Emmanuel.VanLil@ESAT.KULeuven.Be](mailto:Emmanuel.VanLil@ESAT.KULeuven.Be)

R. Van Malderen  
Royal Meteorological Institute  
Ringlaan, 3  
B-1180 Uccle  
BELGIUM  
Email: [Roeland.VanMalderen@Meteo.Be](mailto:Roeland.VanMalderen@Meteo.Be)

# A statistical study of atmospheric circumstances on microwave links.

Emmanuel H. Van Lil<sup>(1)</sup> and Roeland Van Malderen<sup>(2)</sup>

(1) KU Leuven, Heverlee, 3001, Belgium, e-mail: Emmanuel.VanLil@ESAT.KULeuven.Be

(2) Royal Meteorological Institute, Uccle, 1180, Belgium; e-mail: Roeland.VanMalderen@Meteo.Be

## Abstract

In a previous paper [1], we investigated the worst-case scenario of the influence of atmospheric circumstances on the propagation of microwave links. In this document, we will investigate this problem from a statistical point of view. This allows quantifying the probability of unlikely events to happen, and their impact on the quality of the transmission.

## 1. Introduction

The current authorisation criterion imposes that a large area is usually excluded from fixed or moving objects like wind turbines. An example of those zones is shown in Fig. 1.

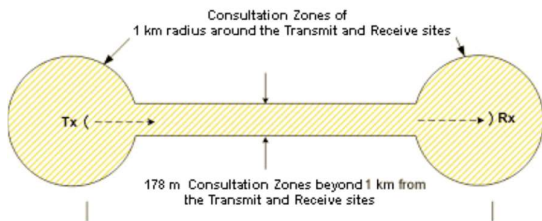


Fig. 1: Consultation zone for a microwave link (from [2])

If those criteria would be strictly enforced, no new high constructions could be allowed in Belgium, as illustrated by a 2004 map (courtesy BIPT-IBPT) of microwave links in Belgium (Fig. 2).

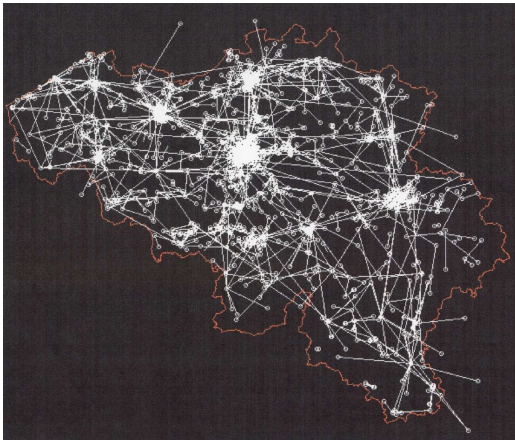


Fig. 2: Microwave links in Belgium (courtesy BIPT)

The trajectory of a microwave link in space is essentially determined by meteorological parameters. The most important are temperature and pressure but also the partial pressure of water vapour has to be taken into account. However, to calculate the trajectory, we also need the derivatives of those parameters with respect to the height above the local ground level.

## 2. Basic theory

Indeed, the refractive index of air is given in the appropriate ITU-R standard [3]:

$$n = 1 + 77.6 * 10^{-6} / T [p - 0.072e + 4810e / T] \quad (1)$$

where  $T$  is the temperature in degrees Kelvin,  $p$  and  $e$  respectively the total pressure and the partial pressure of water vapour, both in hPa. This formula is also used for precision interferometric measurements in a room where temperature, pressure and humidity are kept constant. This is illustrated by the setup of the metrology lab of the Belgian ministry of economy (Fig. 3).

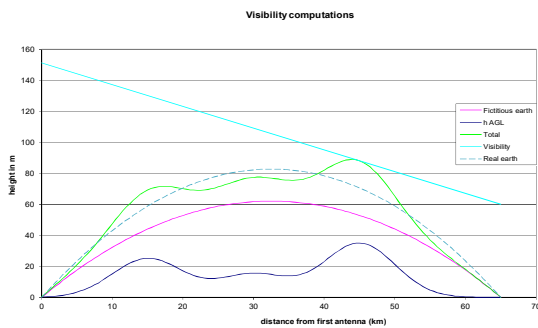


Fig. 3: Belgian interferometric length measurement lab (picture taken at SMD)

The knowledge of the refractive index allows us to follow a wave transmitted over a microwave link if assuming an atmosphere consisting of concentric spheres with a homogeneous refractive index between two consecutive spheres. It has been shown that the equivalent radius of curvature of the path of the wave  $R_{eq}$  is given by [4]:

$$\frac{1}{R_{eq}} = \cos(\psi) \left( \frac{dn}{ndh} + \frac{1}{R_a + h} \right) \quad (2)$$

where  $R_a$  is the local radius of the earth's surface (smaller than 6378137 m in the WGS84 ellipsoid) along the direction of the microwave link,  $h$  is the altitude above the local ground level, and  $\psi$  is the angle of the propagation direction with the tangent plane to the local sphere. Since this angle is very close to  $0^\circ$ , the cosine is approximately one. For the standard atmosphere, the proportion  $K$  between the effective radius and the real radius needed to compute the equivalent height above the cord is about 4/3. In fact, it lowers the profile of the earth so that the radio horizon is further away than the geometrical one. This is illustrated in Fig. 4 for a 65 km link on a fictitious terrain with three artificial mountains.



**Fig. 4:** Fictitious terrain profile with three Gaussian mountains at 15, 30 and 45 km of a 65 km microwave link.

A more realistic profile of a microwave link at 7 GHz with a large wind turbine above the link is shown in Fig. 5. The terrain heights have been obtained from the freely available SRTM (Shuttle Radar Tomography Mission) [5]. The tower is far away from the centre of the link (even if it is not shown on the figure), but, due to the large diameter of the turbine, there is a horizontal overlap with the three Fresnel radii. A cross-section showing the first ellipsoid and the locus of the tips of the turbine is shown in Fig. 6 for the standard atmosphere. In exceptional propagation circumstances (in this case with a negative  $K$  factor) they can become tangent to each other (Fig. 7) and even overlap (values of  $-0.1332 < K < -0.0014$ ).

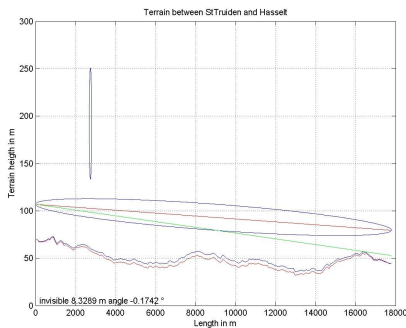


**Fig. 5:** Real terrain profile of a high wind turbine located above a 7 GHz microwave link of 17.8 km. The red line connects the centres of the antennas and the blue ellipse is

the first Fresnel ellipsoid. The terrain without curvature correction is in red, and with standard atmosphere correction in blue, as well as the wind turbine. The green line is the radio visibility of the left antenna.

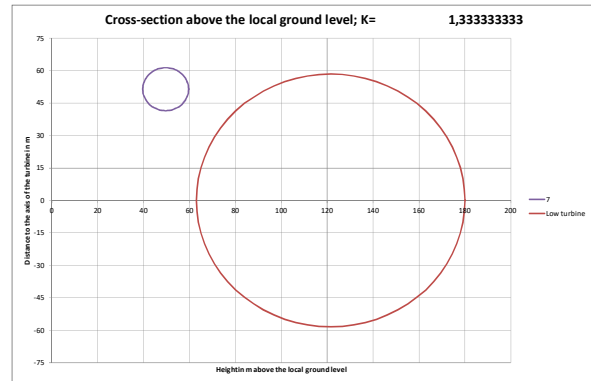


**Fig. 6:** Cross-section of a high wind turbine located above a 7 GHz microwave link at the location of the turbine for the standard atmosphere with  $K=4/3$ . In this and all next plots, the largest circle is the locus of the tips of the turbine and the smaller ones the cross-sections of the first Fresnel ellipsoids of the links.

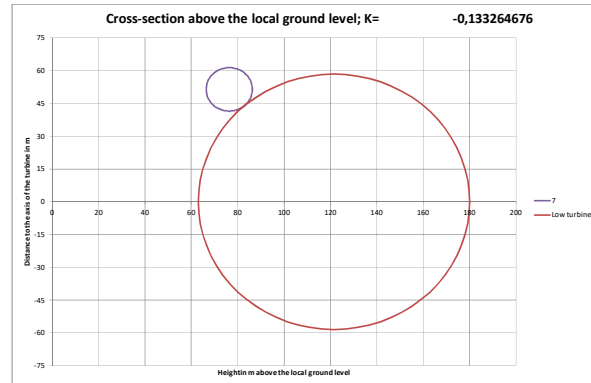


**Fig. 7:** Cross-section of a high wind turbine located above a 7 GHz microwave link at the location of the turbine for a non-standard atmosphere ( $K=-0.1332$ ).

A similar behaviour is valid for two high microwave links above a smaller turbine (at 7 and 12 GHz, with antennas at different heights). In Fig. 8, we notice that the 12 GHz link is - in the worst-case position of the turbine blades - slightly overlapping with the first Fresnel ellipsoid. The approximate formula from ITU-R [6] does not show any attenuation for this small overlap. The antennas of the 12 GHz link could be relocated at a higher position. The first Fresnel ellipsoid touches the locus of the tips of the turbine when  $K=0.84$ , see Fig. 9. At this point, the 12 GHz microwave link has an attenuation of 0.9 dB.

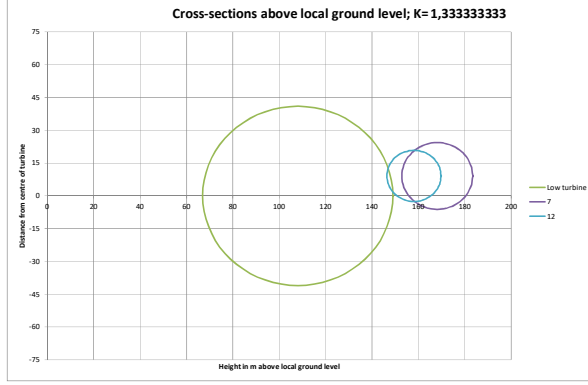


**Fig. 8:** Cross-section of a low wind turbine located below two microwave links (at 7 and 12 GHz, with antennas on the same towers) at the location of the turbine for a standard atmosphere.

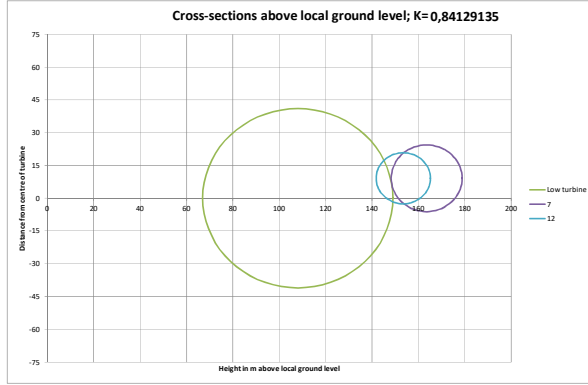


**Fig. 9:** Cross-section of a low wind turbine located below two microwave links (at 7 and 12 GHz, with antennas on the same towers) at the location of the turbine for a non-standard atmosphere ( $K=0.84129135$ ).

For the non-standard atmosphere, the value of  $K$  is, in a very good approximation, for a microwave link ( $h \ll R_a$ ) and  $\psi \approx 0$ , given by:

$$K = R_{eq} / R_a \cong 1 / \left[ 1 + R_a / n \left( \frac{dn}{dh} \right) \right] \quad (3)$$

Assuming the refraction index being one, there is a nice relation between the derivative and the  $K$  factor. It is shown in Fig. 10 .

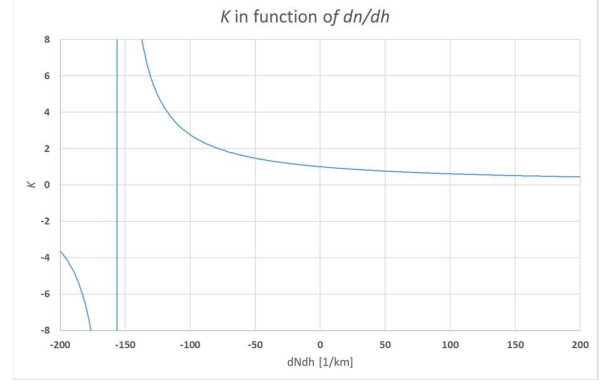


**Fig. 10:** relation between the  $K$  factor and the derivative of the refraction index.

In a previous paper, we have derived worst-case  $K$  factors from meteorological data. We will now start again from the same equation for the derivative of the refraction index with the height above the local ground. We can easily obtain this derivative from Eq. (1):

$$\frac{dn}{dh} = 77.6 * 10^{-6} \left[ \frac{dp}{dh} + (4810/T - 0.072) \frac{de}{dh} - (p - 0.072e + 9620e/T) / T \frac{dT}{dh} \right] / T \quad (4)$$

or

$$\frac{dn}{dh} = ct_1 \frac{dp}{dh} + ct_2 \frac{de}{dh} + ct_3 \frac{dT}{dh} = t_1 + t_2 + t_3 \quad (5)$$

### 3. Discussion of the meteorological measurements

The Royal Meteorological Institute of Belgium (RMI) in Uccle, Brussels, is performing twice daily (until Nov. 2003) or three times a week (after Nov. 2003) measurements with a weather balloon, allowing to retrieve the vertical profile of all needed parameters like the temperature, pressure, and humidity in function of altitude (Fig. 11).



**Fig. 11:** Example of weather balloon (courtesy of RMI)

Here, we use only the measurements by sensors carried by these weather balloons, and not from ground-based devices. The extreme values recorded in the time period 1968-2016 are summarised in Table 1.

**Table 1:** Values of the maxima and minima of the important meteorological parameters at low altitude (the subscript  $s$  denotes surface, or  $h=0$ ) at Uccle, Brussels.

| Variable    | Dimension | Minimum | Maximum  |
|-------------|-----------|---------|----------|
| $T_s$       | K         | 256.050 | 307.150  |
| $p_s$       | hPa       | 946.000 | 1110.400 |
| $e_s$       | hPa       | 0.278   | 29.941   |
| $dT/dh<200$ | K/m       | -0.107  | 0.060    |
| $dp/dh<200$ | hPa/m     | -0.403  | -0.107   |
| $de/dh<200$ | hPa/m     | -0.105  | 0.050    |

All those variables are stochastic functions, as illustrated in Fig. 12, Fig. 13, and Fig. 14 for respectively the temperature, pressure, and the humidity. Those plots show the raw values of the pdf and the cdf, together with a Gaussian approximation. Those raw data files contain all valid measurements; missing data have of course been eliminated in those plots).

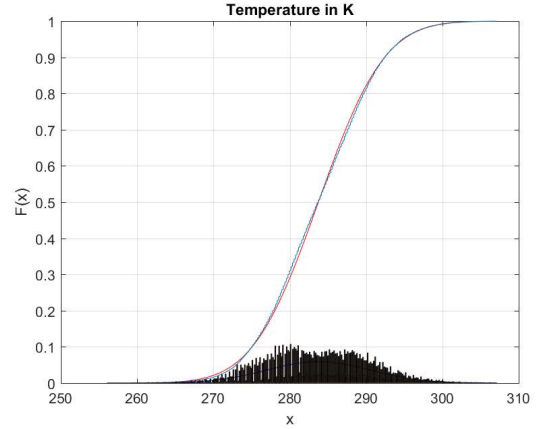


**Fig. 12:** Raw temperature data (27676 valid data points).

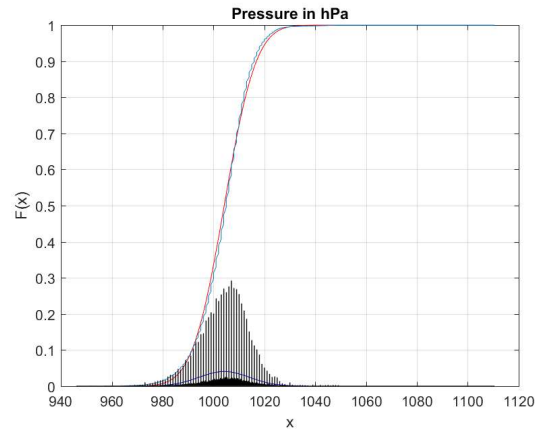


**Fig. 13:** Raw pressure data (27880 valid data points).

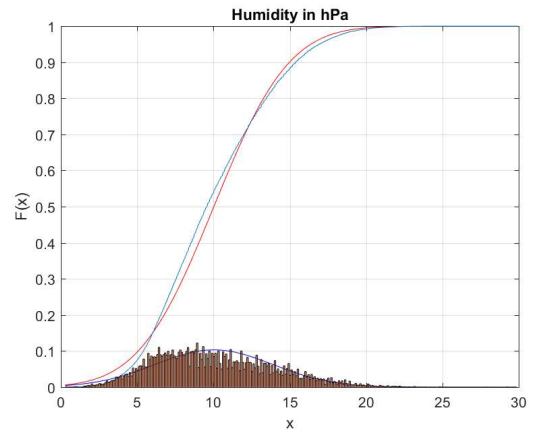


**Fig. 14:** Raw humidity data (25636 valid data points).

Only the humidity density distribution is consistent. The inconsistency present in the density distribution of the pressure and temperature can be ascribed to the use of a different resolution before and after 1/1/1990. From this date, a new type of measurement device (radiosonde) was

introduced for the balloon soundings at Uccle. Indeed, the resolution of the old data is limited to a resolution of one hPa (pressure) and 0.2 degrees centigrade (or Kelvin) for the temperature. After 1/1/1990, the resolution increased to 0.1 hPa and 0.1 degrees centigrade for the pressure and temperature measurements respectively. This leads to a much higher probability of the low-resolution numbers in the dataset. To remove this inconsistency, we have rounded the newer measurements to the lower resolution of the older measurements (nearest values). This approach already gave more consistent distribution functions. Another artefact in the data has also been eliminated. During the first 2 months of 1990, both the new and old measurement devices have been launched with weather balloons, resulting in a dataset with measurements at both resolutions. Those doubles have been eliminated as well.

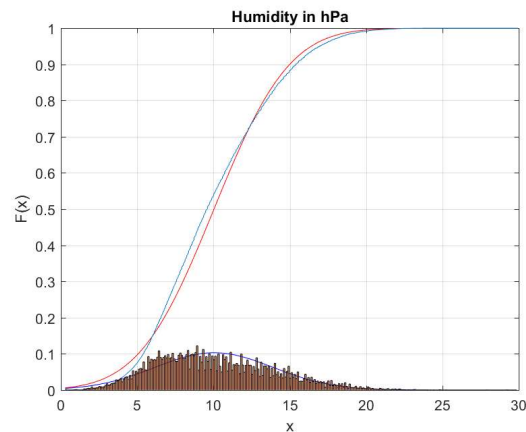


**Fig. 17:** Rounded unique humidity data (25521 valid data points).

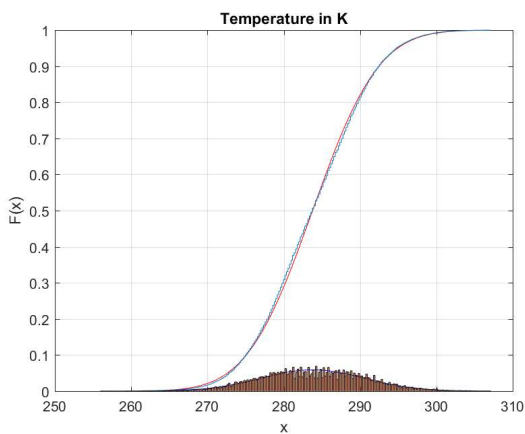


**Fig. 15:** Rounded unique temperature data (27561 valid data points).

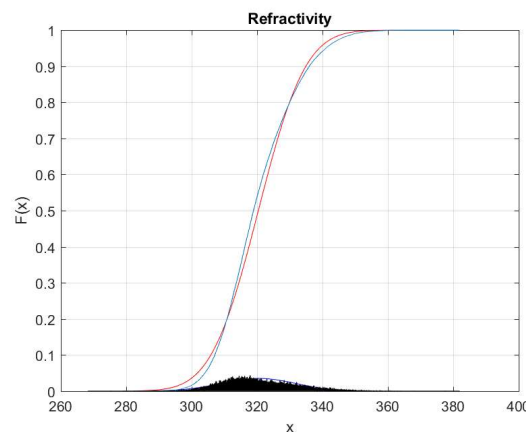


**Fig. 18:** Rounded unique refractivity data (25521 valid data points).

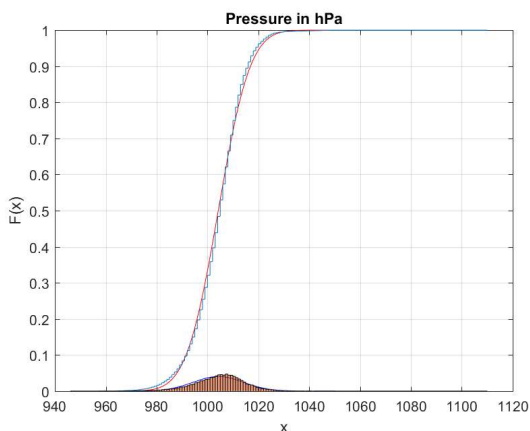


**Fig. 16:** Rounded unique pressure data (27765 valid data points).

Since the humidity dataset was computed from other measurements no extra rounding was needed (just eliminating doubles), as can be seen when comparing Fig. 14 with Fig. 17.

#### 4. Determination of the extreme $K$ values

The maximal value for  $n$  (or the refractivity  $N=(n-1)*10^6$ ) is obviously found by using the maximal pressure values (both for dry air and for the partial pressure of the humid component) and the minimal temperature values:

$$N_{\max} = 77.6 / T_{\min} [p_{\max} - (0.072 - 4810 / T_{\min})e_{\max}] \quad (6)$$

The minimal value is analogously obtained by:

$$N_{\min} = 77.6 / T_{\max} [p_{\min} - (0.072 - 4810 / T_{\max})e_{\min}] \quad (7)$$

The acquired minimal and maximal values for the refractivity are respectively 240.1 and 506.3. They are really worst cases, since in fact  $N$  should be computed for every measurement, since the maximal partial pressure of the water vapour does not occur at the same time as the maximal total pressure. In this case, the extreme  $N$  values would vary between 268.3 and 381.9. For the derivative, it is more complicated, since some values can be negative (apparently, only  $dp/dh$  is always negative in the collected measurements, what is expected from the laws of physics of gases). We have to deal with 3 terms.

We have computed the extreme values for the derivative of the refraction index  $dn/dh$  in [1]. This derivative varies between  $-0.876*10^{-6}$  and  $0.539*10^{-6}$  [1/m]. Note that the value of  $dn/dh$  for the standard atmosphere is  $-0.039*10^{-6}$  [1/m].

Now, we have to fill all the extreme values for  $n$  and  $dn/dh$  in (3) to find the extreme values for the  $K$  factor.

$$K_{\max} \cong 1 / \left[ 1 + R_a / n_{\min} \left( \frac{dn}{dh} \right)_{\min} \right] \quad (8)$$

and

$$K_{\min} \cong 1 / \left[ 1 + R_a / n_{\min} \left( \frac{dn}{dh} \right)_{\max} \right] \quad (9)$$

Note that to obtain the largest  $K$  value, we have to use the smallest denominator. Therefore, since the minimum of  $dn/dh$  is negative, we have to divide  $dn/dh$  by the smallest value of  $n$  (but it does not matter much since  $n$  is close to one). This is also the case for the maximal value. The extreme values for  $K$  are then -0.218 and 0.225. So in extreme conditions,  $K$  can start at 0.225 (bending the wave towards the earth; i.e. substandard atmosphere), then gradually increases over the free space situation with  $K=one$  to the 4/3 of the standard atmosphere over the super standard atmosphere to  $K=+\infty$ . Then  $K$  becomes negative (ducting) and can go up to the value of -0.218. Again, when using values that occurred at the same time, we find less stringent extreme values for  $K$ , i.e. -0.482 and 0.608.

#### 5. Statistical Analysis of the $K$ values

To determine the mean and the variance, we first need the mean and variances of the different parts.

**Table 2:** Values of the mean and variances and minima of the important meteorological parameters at low altitude (the subscript  $s$  denotes surface, or  $h=0$ ) at Uccle, Brussels.

| Variable    | Dimension | Mean      | Variance |
|-------------|-----------|-----------|----------|
| $T_s$       | K         | 283.773   | 6.788    |
| $p_s$       | hPa       | 1004.228  | 9.882    |
| $e_s$       | hPa       | 10.031    | 3.876    |
| $dT/dh<200$ | K/m       | -0.007146 | 0.016203 |
| $dp/dh<200$ | hPa/m     | -0.121156 | 0.011415 |
| $de/dh<200$ | hPa/m     | -0.004510 | 0.013957 |

The easiest way is to compute directly the mean and variance of the valid refractivity values and their derivative. The mean value of the refractivity is 320.4 and its variance is 11.3. The mean value of the derivative of the refractivity is -0.038 [1/m] and its variance is 0.045 [1/m]. Note that the mean is very close to the one of the standard atmosphere. From Eq. (3), we find the values for the mean of the  $K$  factor, using the fact that for independent stochastic values  $E(xy)=E(x)E(y)$ . As we expect, the mean of the  $K$  factor is close to the value of the standard atmosphere, i.e. 1.3239. A direct computation of  $K$  would lead to different results, since  $K$  can become infinite in the case of ducting (as can be seen in Fig. 10). Taking mean and variance of  $1/K$  solves this anomaly. They are respectively 0.75525 and 0.28725, leading to a mean  $K$  of 1.3241. This allows us to claim that the limit case for Fig. 7 lies outside a single sided deviation of -28.75 times the variance, or a nearly zero (much less than  $10^{-180}$ ) probability. The computation of the variance from Eq. (3) is a little bit more complex. From probability theory [7] we should compute the variance from:

$$\sigma^2(xy) = [\sigma^2(x) + E^2(x)][\sigma^2(y) + E^2(y)] - E^2(x)E^2(y) \quad (10)$$

For  $1/K$ , the value computed with this formula is as expected (0.28716).

#### 6. Application to the microwave links

Taking into account those extreme  $K$  values, it is now obvious that the good working of the second microwave link could not be guaranteed in all circumstances. Indeed, from the cross-section (Fig. 19), we notice that the blades could nearly completely shadow the link (the blades do not cover the diameter of the first Fresnel ellipsoid (15.28 m) completely).

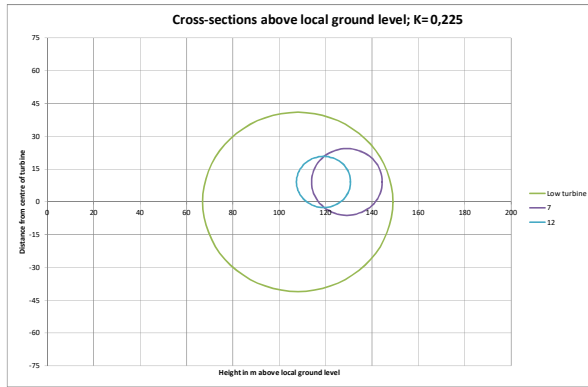


**Fig. 19:** Cross-section of a low wind turbine located below two microwave links (at 7 and 12 GHz, with antennas on the same towers) at the location of the turbine for the worst case atmosphere ( $K=0.225$ ).

The first microwave link however looks much better (Fig. 20) now: the wave will never deviate as much as in Fig. 7. The behaviour of the cross-section of the Fresnel ellipsoid is as follows: for small positive  $K$  values (large positive  $dn/dh$  values), the wave is bent towards the surface of the earth), When  $dn/dh$  decreases and eventually becomes negative the link moves up ( $K$  then switches from  $+\infty$  to  $-\infty$  and continues to increase (or decrease in absolute value)).

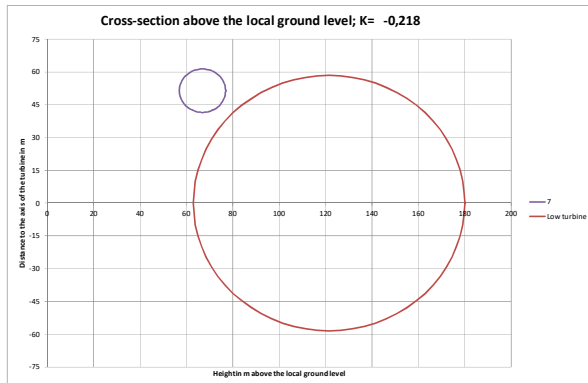


**Fig. 20:** Cross-section of a high wind turbine located above a microwave link at the location of the turbine for the worst case atmosphere ( $K=-0.218$ )

We can also claim that the link would satisfy more stringent criteria like the third Fresnel ellipsoid, but unfortunately not 3x the radius of the first ellipsoid (Fig. 21).

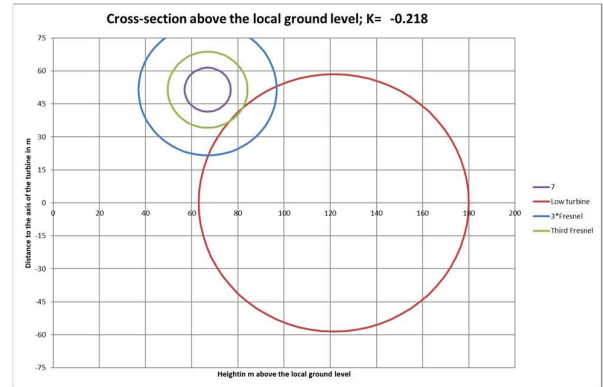


**Fig. 21:** Cross-section of a high wind turbine located above a microwave link at the location of the turbine for the worst case atmosphere ( $K=-0.218$ )

## 7. Conclusions

We have now added a statistical analysis (from  $K$  values) to a worst-case analysis of terrestrial microwave links based on meteorological data available above the location of the Royal Meteorological Institute of Belgium in Uccle (Belgium). This might help in trying to implement green energy, generated by wind turbines, without influencing actual microwave links.

## 8. Acknowledgements

We are greatly indebted EDF-Luminus for the examples of the links.

## 8. References

1. E. Van Lil, R. Van Malderen, "On the worst case trajectories of microwave links above Belgium". Proceedings of the second Atlantic Radio Science conference AT-RASC 2018; 2018; Vol. 2; iss. 1; pp. 1 - 4 Publisher: URSI; Ghent
2. Radio Advisory board of Canada, "Technical Information and Coordination process Between Wind Turbines and Radiocommunication and Radar systems". Can be downloaded (8/1/2018) from: <https://www.rabc-cccr.ca/about/publications/wind-turbines-radio-radar>
3. ITU-R, recommendation P.453-11, "The radio refractive index: its formula and refractivity data", 07/2015
4. Enrique Fernandez and Marc Mathieu, "Les faisceaux Hertiens analogiques et numeriques", Bordas/CNET-ENST, Paris, 1991, ISBN 2-04-018737-5
5. <https://www2.jpl.nasa.gov/srtm/>
6. ITU-R, recommendation P.526-13, "Propagation by diffraction", 11/2013
7. William Feller, "An Introduction to Probability Theory and Its Applications", Vol. 1, 1968, 3rd Edition, John Wiley, New York, ISBN-13: 978-0471257080